EPA-650/2-73-030

October 1973

ENVIRONMENTAL PROTECTION TECHNOLOGY SERIES

INSTRUMENT TO MONITOR CH_4, CO, AND CO_2 IN AUTO EXHAUST

Office of Research and Development
U.S. Environmental Protection Agency
Washington, D.C. 20460

EPA-650/2-73-030

INSTRUMENT TO MONITOR CH_4, CO, AND CO_2 IN AUTO EXHAUST

by

D. E. Burch and J. D. Pembrook

Philco-Ford Corp.
Aeronutronic Division
Ford Road
Newport Beach, California 92663

Contract No. 68-02-0587
Program Element No. 1AA010

EPA Project Officers: J. Sigsby and F. Black

Chemistry and Physics Laboratory
National Environmental Research Center
Research Triangle Park, N. C. 27711

Prepared for

OFFICE OF RESEARCH AND DEVELOPMENT
U.S. ENVIRONMENTAL PROTECTION AGENCY
WASHINGTON, D. C. 20460

October 1973

This report has been reviewed by the Environmental Protection Agency and approved for publication. Approval does not signify that the contents necessarily reflect the views and policies of the Agency, nor does mention of trade names or commercial products constitute endorsement or recommendation for use.

ABSTRACT

An infrared analyzer employing gas cell correlation techniques and thermoelectrically cooled photodetectors has been designed and constructed to measure the concentrations of methane, carbon monoxide, and carbon dioxide in automotive exhausts. The dynamic range from the minimum detectable concentration to the maximum concentration that can be measured accurately for each gas is: methane, 0.3 ppm to 10,000 ppm, carbon monoxide, 0.5 ppm to 10,000 ppm, and carbon dioxide, 10 ppm to 250,000 ppm. The wide dynamic range is made possible by employing two different sample cell lengths for each gas. The concentrations of the three gases are measured simultaneously and independently. Discrimination against other gases in the automotive exhaust is very good.

This report was submitted in fulfillment of contract number 68-02-0587 by Philco-Ford Corporation, Aeronutronic Division, under the sponsorship of the Environmental Protection Agency. Work was completed as of August 1973.

CONTENTS

		Page
Abstract		iii
List of Figures		v
Acknowledgements		vi
Sections		
I	Conclusions and Recommendations	1
II	Introduction	3
III	Optics	12
IV	Electronics	21
V	Test Data	29
VI	Glossary of Symbols	36
VII	Patent Information	39

FIGURES

No.		Page
1	Block diagram of a single gas analyzer	5
2	Rotating gas correlation cells	6
3	Calculated spectral plots of transmittance for a model spectrum similar to a portion of a CO band	8
4	Calculated spectral plots of transmittance demonstrating the response of the gas correlation system to a gas other than the one to be detected	10
5	Schematic diagram of the optics assembly	13
6	Expanded view of slit assembly S2 or S3	18
7	Power supply unit above a single electronics unit	22
8	Schematic illustration of a single channel of the photodetector electronics within the optics assembly	24
9	CO detection sensitivity	30
10	CH_4 detection sensitivity	31
11	CO_2 detection sensitivity	32

ACKNOWLEDGEMENTS

We wish to give special recognition to the ingenuity of Mr. F. J. Gates, a member of our research team. He devoted much of his own time to the development of the instrument and to the testing of its performance.

We appreciate the cooperation and the candor of EPA technical personnel, particularly Mr. F. M. Black in discussions about the instrument and its specifications. The EPA personnel at Raleigh-Durham, North Carolina also furnished us with an analyzed sample of lead-free gasoline for testing the instrument.

SECTION I

CONCLUSIONS AND RECOMMENDATIONS

This program has been completed successfully. An instrument has been designed, constructed, and tested. All the major design criteria were met. The instrument can measure CH_4, CO, and CO_2 simultaneously and independently.

The measurement range includes gas concentrations that vary approximately from those of room air to those of raw automotive exhaust. The system has very good discrimination against other gases that occur in automotive exhausts. Water vapor is the only gas that interferes enough to consider a correction factor to the measurements of CO, CH_4, and CO_2. If the exhaust gas sample contained 3% water vapor, the maximum error resulting from it would be 0.6 ppm (part-per-million) of CO, 2.3 ppm of CH_4, and 30 ppm of CO_2. The concentration of water vapor in the sample can easily be determined, or estimated, to within $\pm 0.5\%$. Thus, the maximum error, in the measurements due to water vapor can be reduced with a correction factor to 0.1 ppm for CO, 0.4 ppm for CH_4, and 5 ppm for CO_2.

The large dynamic range of the instrument necessitates the use of two different sample cell lengths for each gas. Cells of two lengths are active at all times for the CO and CH_4 systems. The operator selects between the two photodetector outputs from the two cells with a switch. Electronic automatic ranging could be incorporated into the instrument.

In the CO_2 system, only one of the two sample cells is in the optical path at a time. A bi-stable mechanical cell position device allows the operator to select between and reposition the cells in a few seconds. Only one photodetector is required for this system.

The spectral passbands of the CO and CH_4 channels of this instrument are defined with a moderately complex grating-filter assembly. This assembly allowed the passbands to be adjusted and selected for good sensitivities to CO and CH_4 and very good discrimination against other gases. If the requirements on discrimination were relaxed, the optics assembly could be simplified by employing other methods of defining the spectral passbands.

If only one sample cell length were required at a time for the CO and CH_4 systems, then the optical throughput of these systems could be increased. This would result in an increase in the signal-to-noise levels of these channels. Further, only one photodetector would be required for each channel. A single cell device would have a dynamic range that is an order of magnitude less than that of the present instrument. The CO_2 system demonstrates one technique for mechanically switching between two sample cells. Similar techniques could allow switching between three or more cells of different lengths for extended dynamic ranges.

The photodetector output signals of each channel are processed independently by three separate electronics units that are almost identical to each other. This modular construction technique allowed thorough testing of the first unit before design approval and construction of the subsequent units. If one electronics unit becomes inoperable, either of the remaining units can be substituted. The total volume occupied by the electronics could easily be halved by repackaging the three electronic units into a single cabinet. If this were done, the parts count could also be reduced by about 25 percent by using a single power supply and reference amplifier.

SECTION II

INTRODUCTION

PERFORMANCE

This section presents sufficient detail for a general understanding of how the exhaust gas analyzer functions. The operational characteristics are summarized. This is followed by a general description of the optics and the electronics. The spectral principles of operation are described in the last portion of this section. Subsequent sections present detailed descriptions of the instrument, its operation, and its calibration and performance.

The exhaust gas analyzer provides for the simultaneous measurement of CO, CH_4, and CO_2. The concentrations of the individual gases are analyzed with a three-channel gas correlation spectrometer. The output signal is proportional to the absorber thickness of the sample gas, which is the product of the concentration of the gas species being measured and the sample cell length under the fixed conditions of room temperature and one atmosphere pressure. Each channel employs two sample cells of different lengths to extend the useful measurement range. The CO and the CH_4 systems have common sample cells. Either system may use either or both cells at any time. All of the photodetectors are thermoelectrically cooled.

With a 1 second time constant on the most sensitive ranges, the minimum detectable gas concentrations are approximately 0.3 ppm (parts-per-million) of CH_4, 0.5 ppm of CO, and 10 ppm (0.001%) of CO_2. The maximum gas concentrations that can be measured reliably are 10,000 ppm of CH_4, 10,000 ppm of CO, and 250,000 ppm (25%) of CO_2. The gas correlation system offers very good discrimination between the gases being measured and other gases that occur in automotive exhaust. The system is also insensitive to particulates in the sample, dirty windows, and changes in source brightness.

EQUIPMENT DESCRIPTION

All three channels of the instrument are similar. Many of the component parts are shared. For clarity, the following description is limited to a single channel. Figure 1 is a block diagram of any channel of the device. Radiant energy from an infrared source is imaged on a photodetector through a chopper, the rotating gas correlation cells, one of two sample cells, and a narrow bandpass filter. Optical components between the source and the photodetector were selected and arranged to give good stability along with a large throughput. The energy is chopped at 360 Hz (Hertz) by an opaque, 12-bladed, chopper deposited on the entrance window of the rotating correlation cells. Figure 2 shows an exploded view of the correlation cells. One of the cells GC2, is filled with a non-absorbing gas and has a neutral attenuator deposited on the window of this cell. The other cell, GC1, is filled with gas of the species being detected. Sufficient gas is placed in this cell to cause equal attenuation by both cells over the spectral bandpass defined by the filter in front of the photodetector. The narrow bandpass filter assembly may be a simple interference filter or a more complex monochromator. The complexity of this assembly is determined by the requirements of sensitivity to the gas species of interest and the rejection of, or insensitivity to, other gases that may be present in the unknown sample gas. The sample gas flows continuously through the sample cell to minimize errors that could be caused by adsorption or desorption of gas on the sample cell walls.

The gas-filled correlation cells rotate at 1800 rpm, which has the effect of switching the optical path between the corrolation cells at 30 Hz. When no sample is present in the sample cell, the photodetector output consists of a 360 Hz carrier signal due to the 360 Hz chopper. When the sample cell contains gas of the same species as the gas in the correlation cell, the photodetector output consists of a 360 Hz carrier modulated at 30 Hz. The amount of 30 Hz modulation is proportional to the absorber thickness of the detected gas present within the sample cell. Thirty Hz modulation to the carrier occurs only when the sample gas absorbs energy within the system's spectral bandpass. Further, for modulation to occur, the absorption must correlate to some extent with the absorption characteristics of the gas within the gas correlation cell. Placing a neutral attenuator within the sample cell would not cause 30 Hz modulation since both halves of the correlation cell cycle would be affected equally.

The carrier may exhibit 30 Hz modulation when no sample is present if one correlation cell window collects more dust than the other or if the temperature of the correlation cell changes. Since these events are certain to occur, no attempt was made to achieve perfect balance between the cells. Instead, an electronic 30 Hz modulator is employed to cancel any residual modulation that occurs.

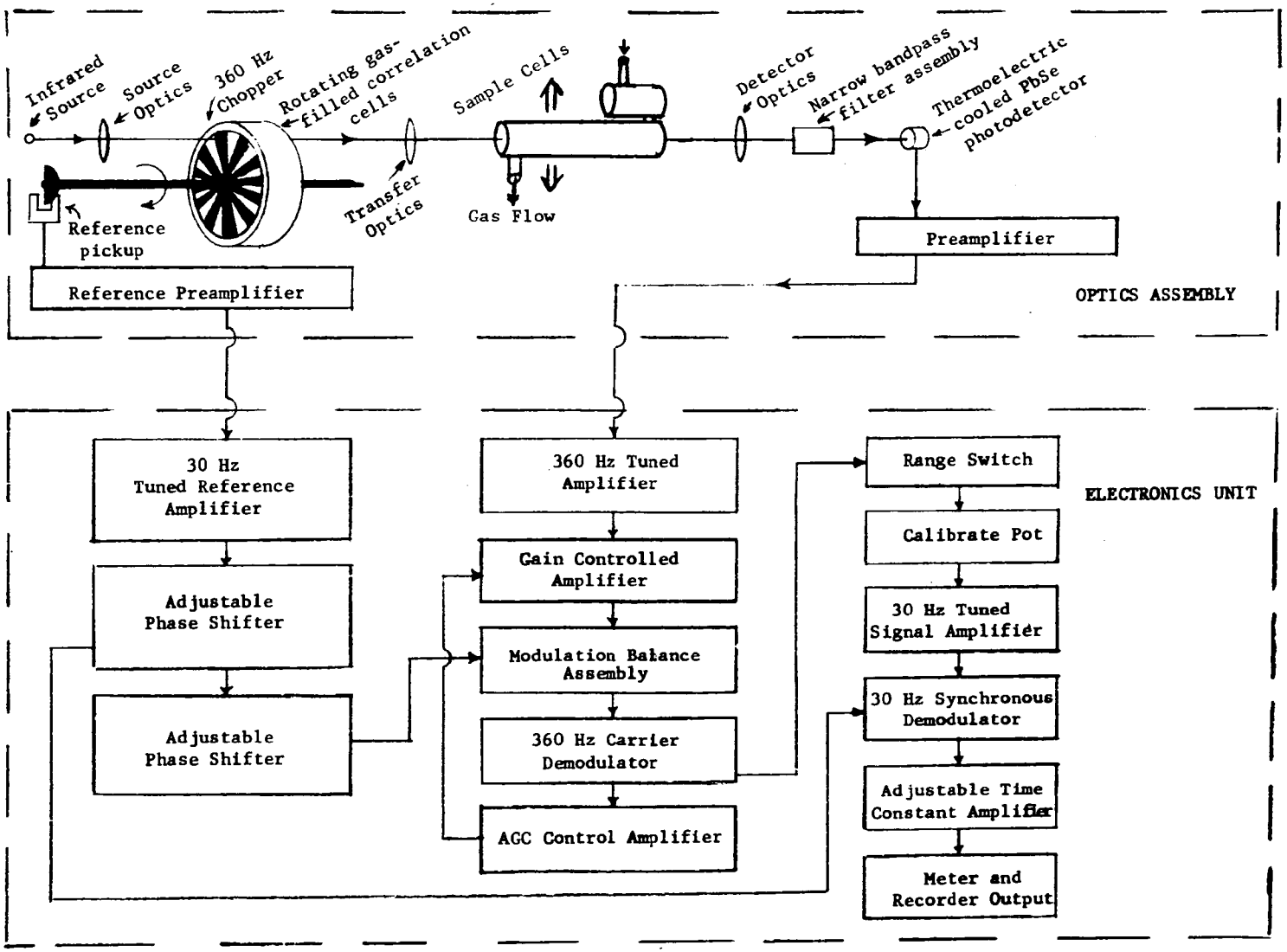

Figure 1. Block diagram of a single gas analyzer.

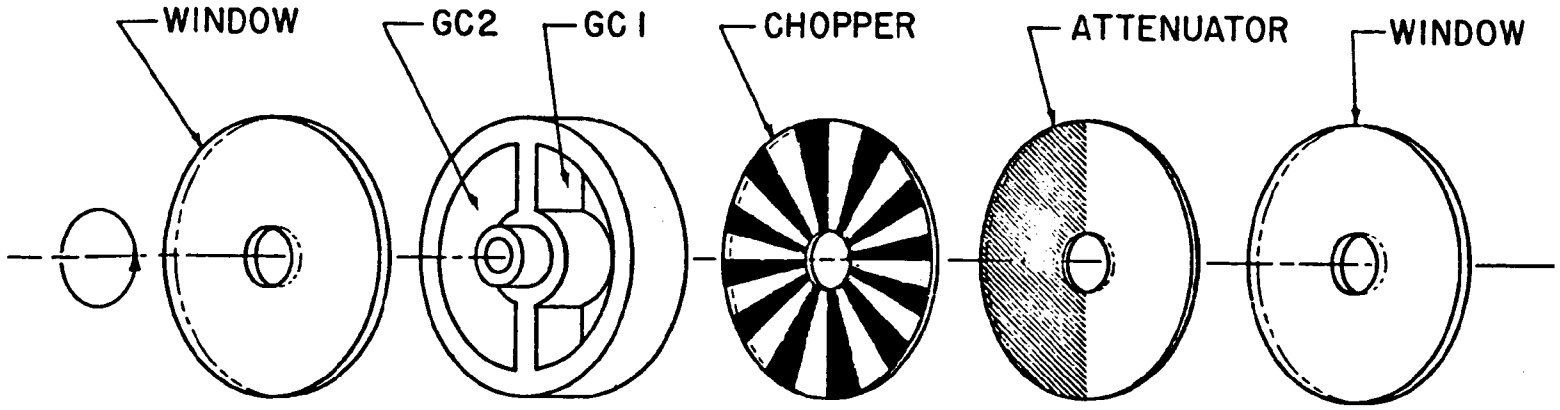

Figure 2. Rotating gas correlation cells. Windows are antireflection overcoated sapphire.

SPECTRAL RESPONSE

The spectral sensitivity of the gas correlation spectrometer is set by the narrow bandpass filter and by the absorption characteristics of the gas in the gas correlation cell. The CO detection system is used to illustrate the operating principles. The use of the carrier at a frequency, f_c, of 360 Hz does not affect the spectral sensitivity of the instrument. If the carrier chopper were removed from the system shown in figure 1, the detector output would occur at the frequency, f_a, of 30 Hz. During one half the cycle GC2 would be in the beam; during the other half cycle the gas filled correlation cell, GC1, would be in the beam.

Figure 3 contains several calculated plots of transmittance that can be used to explain the spectroscopic principles of detection. We have assumed certain gas sample parameters and have chosen a band model consisting of two absorption lines with spacings, strengths, and half-widths typical of the stronger lines of the fundamental CO band. The half-widths at 1 atmosphere pressure are 0.08 cm^{-1}; strength = 2π; and the lines are separated by 4 cm^{-1}. Correlation cell GC1 is assumed to contain 0.2 atm cm of CO at a total pressure of 1 atm. Its transmittance spectrum over the region of the calculation is shown in the upper portion of figure 3 and is indicated by T_1. We note that this sample is essentially opaque ($T_1 = 0$) near the centers of the two absorption lines. We assume that the bandpass filter passes only the spectral region from $(\nu - \nu_a) = 0$ to 4, which corresponds to the region between the centers of the lines.

The attenuator on GC2 is a netural density filter with constant transmittance, T_2, equal to the average transmittance of the CO in correlation cell GC1 over the bandpass of the filter. The third curve in the upper panel of the figure is a plot of the difference between the other two transmittance curves. This curve represents the spectral response of the system. Since T_2 is equal to the average of T_1, the integral of the curve $(T_2 - T_1)$ is 0. Thus, with no sample in the sample cell, no voltage component V_a is produced as the rotating cells move first GC1 and then GC2 into the beam.

We now consider a sample cell containing enough CO to produce the transmittance spectrum indicated by the center panel of figure 3. This corresponds to two of the stronger CO lines with an absorber thickness of 0.01 atm cm at a pressure of 1 atmosphere. When GC1 is in the beam, the spectrum after the beam has passed through the sample is given by the product of the transmittances $T_1 \times T_{sam}$. This is indicated by the curve in the lower panel of figure 3 along with the corresponding curve that applies when the beam is going through GC2. The resulting detector signal, V_a, is proportional to the difference between the two integrals

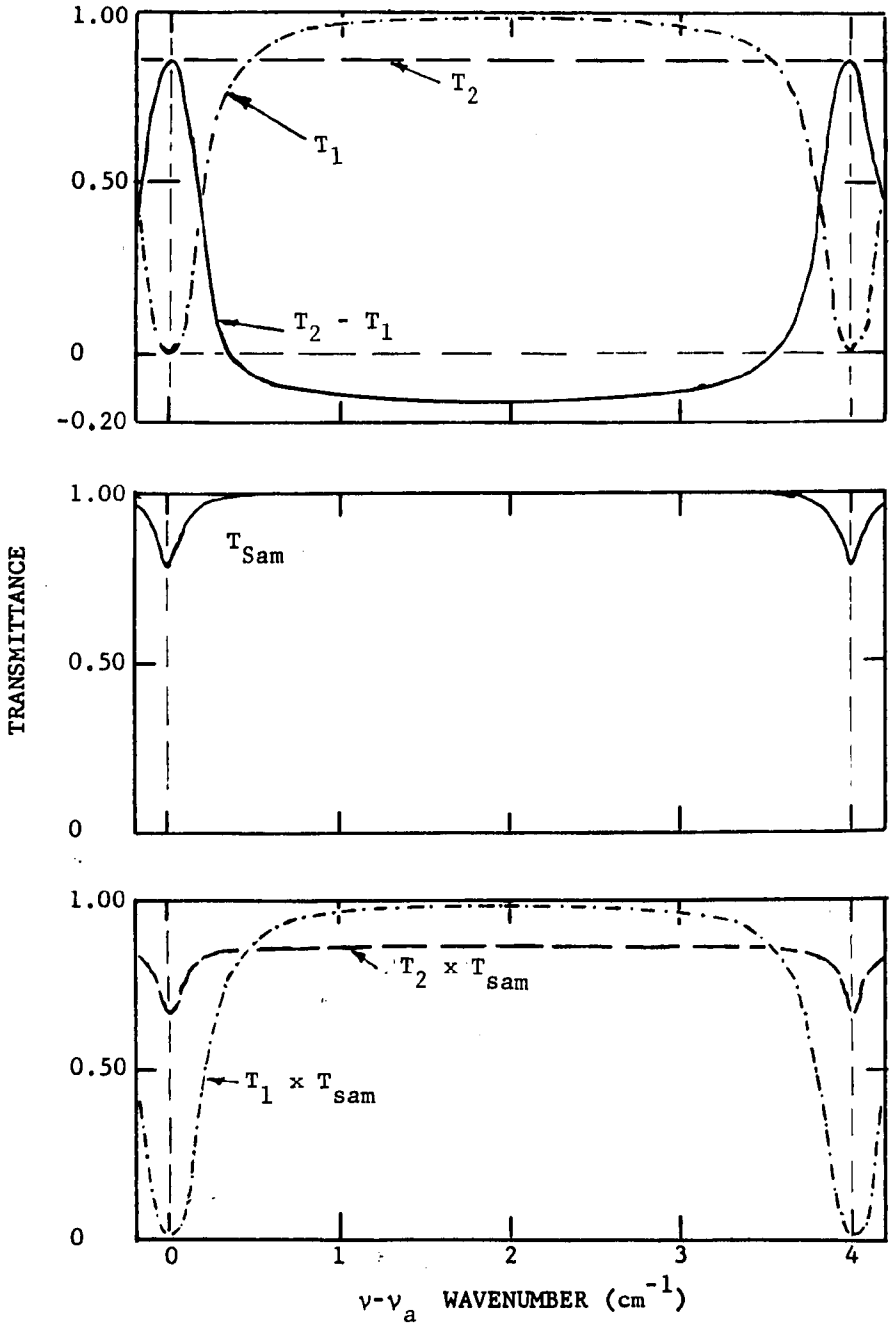

Figure 3. Calculated spectral plots of transmittance for a model spectrum similar to a portion of a CO band. The wavenumber scale is measured from the center of one of two identical lines. The curves illustrate the spectral principle of operation of a gas analyzer using one gas correlation cell filled with the gas species being measured and an attenuator with a flat response whose absorptance is equal to the average absorptance of the gas correlation cell.

$\int(T_1 \times T_{sam})\, d\nu$ and $\int(T_2 \times T_{sam})\, d\nu$. The value of the first integral is 3.424 cm^{-1}, and the latter one is approximately 0.5% less. Thus, the presence of the CO in the sample cell has produced a detector signal V_a at a frequency f_a that is approximately 0.5 percent of the signal that would result if the beam through GC2 were blocked. The sample absorbs a smaller fraction of the beam that passes through GC1 than the beam that passes through GC2. This occurs because there is very little energy left in the beam through GC1 at wavelengths where the sample can absorb. It is clear that V_a will increase with increasing amount of CO in the sample cell until the absorption in the sample is approximately as much as that in cell GC1.

Figure 4 shows a similar set of curves for a sample that contains no CO but does contain another gas with a spectral line between the CO lines as indicated in the center panel. The lower panel shows a curve that corresponds to the response of the system times the transmittance of the sample. This sample produces a detector signal that corresponds to a negative amount of CO. The spectrum of this gas has negative correlation with the spectrum of CO. As shown by the transmittance curves, the sample absorbs most where the CO absorbs least, and vice-versa.

Recall from the discussion of the upper panel of figure 3 that the average value of $(T_2 - T_1)$ is 0; thus, a gas that absorbs a constant amount over the spectral band will not produce any detector signal V_a at frequency f_a. Most gases that absorb in the infrared contain many vibration-rotation absorption lines so that the absorption is not constant over an interval a few cm^{-1} wide. If the strengths and the positions of the lines of a gas are completely at random with respect to the lines in the spectrum of CO, the absorption by that gas will not produce a signal at frequency f_a. In this situation, the influence of the lines that occur in regions where $(T_2 - T_1)$ is positive are exactly cancelled by those lines that occur where this quantity is negative, and the interfering gas absorbs the same fraction of the beams through both GC1 and GC2.

Consider a sample consisting of both CO and an interfering gas with spectra that are completely uncorrelated. This condition of no correlation is described mathematically by:

$$\frac{1}{\Delta\nu}\int T_\chi \times T_{CO}\, d\nu = \frac{1}{\Delta\nu}\int T_{CO}\, d\nu,$$

where $\Delta\nu$ is the spectral bandpass, and T_χ and T_{CO} are the transmittances of the sample gases χ and CO, respectively. Positive correlation exists when the left-hand side of the above expression is greater than the right-hand side. The opposite is true for negative correlation. The absorption by the interfering gas changes the voltage V_a produced by the CO, although the interfering gas would produce no voltage if it were alone

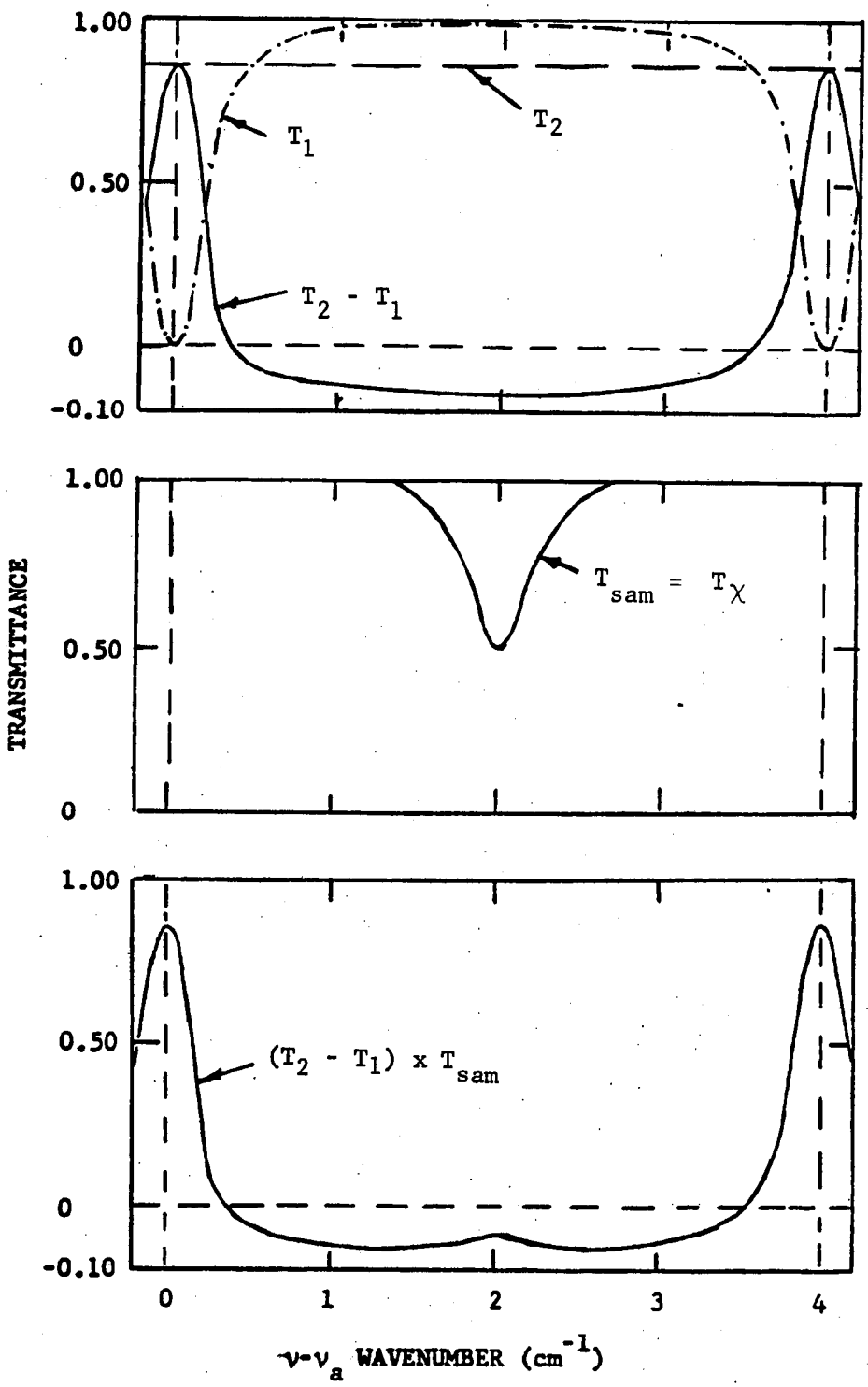

Figure 4. Calculated spectral plots of transmittance demonstrating the response of the gas correlation system to a gas other than the one to be detected.

in the sample. For example, if $\bar{T}_x$, the average transmittance of the interferring sample is 0.8, the voltage V_a produced by the CO is reduced to 0.8 of its correct value. It follows that changes in source brightness or detector sensitivity would also change V_a accordingly.

We now reconsider the system illustrated in figure 1 with the chopper operating at a carrier frequency f_c. The detector signal, V_c, at frequency f_c is proportional to $\int T_2 \times T_{sam}\, d\nu$ when GC2 is in the beam and is proportional to $\int T_1 \times T_{sam}\, d\nu$ when GC1 is in the beam. The sum of these two integrals, $\int (T_1 + T_2)\, T_{sam}\, d\nu$ is proportional to V_c, averaged over a complete cycle of the pair of rotating cells. Absorption by an uncorrelated interfering gas reduces V_c by the same fraction that it reduces V_a, which is proportional to $\int (T_2 - T_1) T_{sam}\, d\nu$. Thus the ratio V_a/V_c is unchanged by an interfering gas that is uncorrelated with the CO, or by variations in source brightness or detector sensitivity. The signal of primary importance is therefore V_a/V_c, since it is a measure of the amount of CO gas and is insensitive to the variations that produce serious errors in many systems.

An electronic circuit designed to measure V_a/V_c is shown in figure 1. When correlation exists between the absorption spectra of the sample and the absorption spectra of the gas within the correlation cell, the carrier is modulated at 30 Hz. The phase of the modulation depends on whether the correlation is positive or negative. Since a synchronous demodulator is used in the electronics, the presence of certain sample gases may result in a negative signal output.

To simplify the measurement of V_a/V_c, an AGC (automatic gain control) is employed within the electronics. Both V_a and V_c are amplified by the gain controlled amplifier. The gain of this amplifier is continuously adjusted by the AGC to hold the average value of V_c constant. The V_a component of V_c is directly proportional to the ratio V_a/V_c when V_c is held constant. The system is calibrated in terms of signal output with the AGC operating versus the absorber thickness of the gas within the sample cell. The calibration is performed with a flowing gas sample at one atmosphere pressure and at room temperature; the absorber thickness is proportional to the gas concentration for a given sample cell length.

SECTION III

OPTICS

GENERAL DESCRIPTION

The three-channel gas correlation spectrometer optics assembly was designed for good stability and large throughput while preserving a reasonably small package size and weight. The selection of optical components was limited to off-the-shelf items wherever possible. First surface mirror optics were used exclusively to eliminate chromatic aberation. All imagery is performed with spherical mirrors. All of the windows are sapphire and are antireflection coated to reduce reflection losses and optical intereference between window surfaces. Apertures reduce scattered energy; some are overfilled to increase stability. Components are arranged to minimize alignment errors that could result from flexure in the baseplate or from differential expansion due to thermal gradients. Except for the source, all components that can be removed are either self aligning or do not require alignment. All other components are bonded in place. The system may either be used horizontally on a bench or mounted vertically within an electronics rack. The overall dimensions of the basic optics assembly as used on a bench top are about 39 cm wide by 25 cm high by 100 cm long. Angle brackets attached to the instrument sides with rubber loaded bolts allow the optics assembly to be mounted in a standard 19-inch (48.3 cm) electronics rack.

A schematic diagram of the optics assembly is presented in figure 5. The three-channel system has two major subdivisions; the CO_2 system and the CO and CH_4 systems. Only the motor, the Nernst source, the reference pickup, and the bias battery are shared by these two subsystems. Each of these subsystems is further divided into the subassemblies presented in figure 1 for a single channel system.

SOURCE ASSEMBLY

A single infrared source is shared by all three channels of the gas correlation spectrometer. The Nernst glower source has a relatively high radiant emittance in all three spectral regions. It also has good

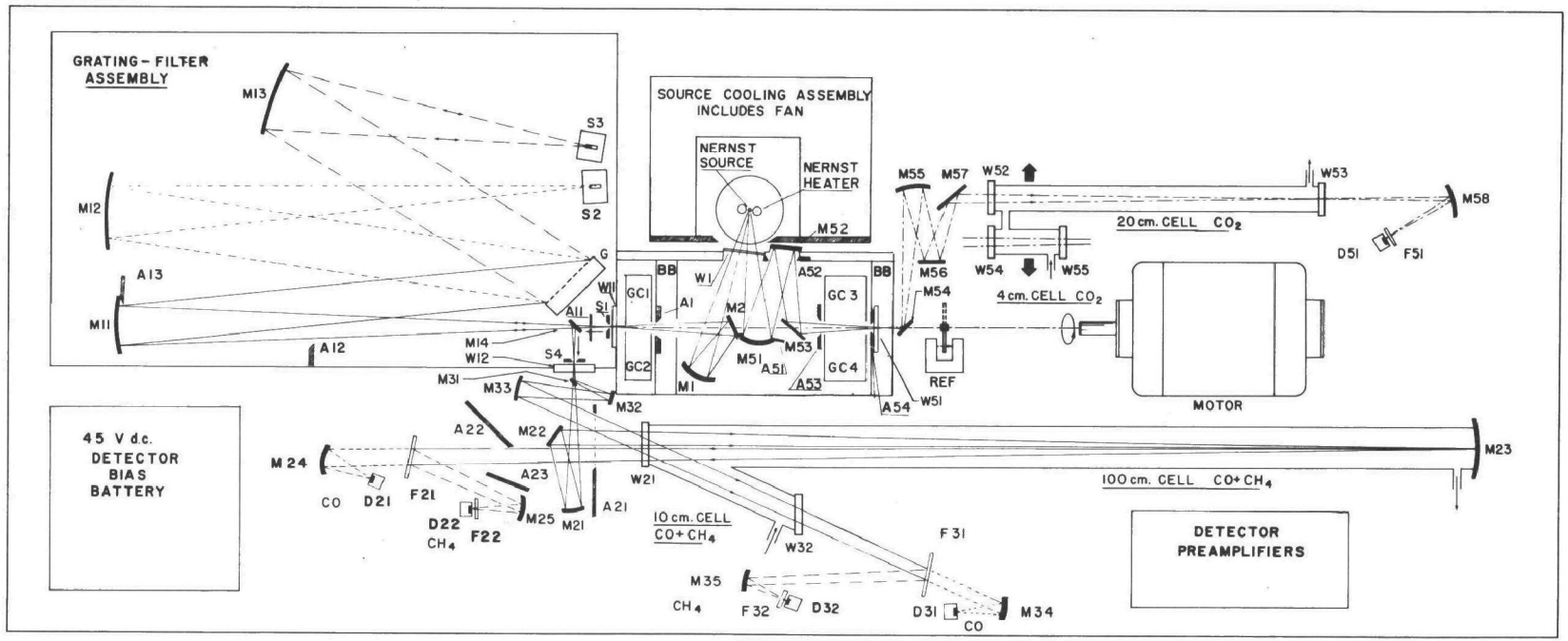

Figure 5. Schematic diagram of the optics assembly.

The components are numbered as a mirror M, window W, thermoelectrically cooled photodetector D, filter F, plane diffraction grating G, aperture A, slit S, gas correlation cell GC, or bearing block BB.

stability and long life, and is easy to use. The standard source mount has been mounted on an assembly that allows transverse adjustment for proper alignment of the source.

The source dissipates about 60 watts of power during normal operation. The source is surrounded by a double walled box. A fan forces room air through the box between inner and outer walls to keep the system cool. Gaskets prevent the cooling air from leaking into the optical path. The cooling assembly is thermally isolated from the remainder of the optics unit. The cooling assembly has been black anodized to increase its emissivity and absorptivity. The wall that separates the source from the gas correlation cell assembly has been mirrored to reflect heat back into the source cooling assembly. The power dissipation of the source is reduced to about 18 watts when the source is operated in the standby mode. The fan speed is reduced during this mode of operation to prolong the fan lifetime.

GAS CORRELATION CELL ASSEMBLY

An exploded view of a set of rotating gas correlation cells is presented in figure 2. The cells are pinned to an axial shaft that is driven at 1800 rpm by a synchronous motor. This has the effect of switching the optical path between the cells at 30 Hz. Energy from the source is chopped at 360 Hz with an opaque 12-bladed chopper that is deposited on the entrance window of the rotating cells. The 360 Hz chopper is on the source side of the gas correlation cells to minimize scattered energy within the cells. Cell GC2 contains a non-absorbing gas, N_2, and has a metallic coating of about 70% transmittance deposited on one window. Cell GC1 contains 5% N_2 as well as the two gas species being detected, 32% CH_4 and 63% CO at a total pressure of 0.71 atm. The concentrations and the total pressure were chosen so that the transmittances of the CH_4 and the CO over the corresponding spectral band passes matched that of GC2. The lengths of GC1 and GC2, 1 cm, were selected so that the total pressure of the mixture in GC1 that balanced the transmittance of GC2 was somewhat less than 1 atm. The construction of the cells is simplified by keeping the internal pressures below atmospheric pressure. The windows are pressed against the bond type seal between the window and the cell body by the pressure gradient. Optimum performance is normally achieved when the gas pressure in GC1 is equal to or somewhat less than the pressure of the sample being studied. However, the effect of changing the total pressure by as much as a factor of 2 is slight provided the concentrations of the CH_4 and CO are adjusted to balance the transmittance of GC2.

A similar pair of correlation cells is used for CO_2. Cell GC3 contains 0.66 atm of pure CO_2 and GC4 contains N_2 at approximately the same pressure. These cells are 2 cm long. One window of GC4 is coated with an attenuator similar to that on the window of GC2. The gas correlation

cells are contained within a dustproof chamber that is sealed with a flexible foam gasket to prevent an accumulation of dust on the cell windows.

A single-bladded chopper pinned to the correlation cell shaft interrupts a beam of light between a light emitting diode and a phototransistor. The 30 Hz output of the phototransistor is used as a reference source to allow synchronous demodulation of the 30 Hz detector signals.

The motor shaft is connected to the gas correlation cell shaft with a flexible coupling. The motor and the bearing blocks BB are pinned to the baseplate to maintain proper alignment. The motor is mounted within a chamber in the optics assembly. Room air is drawn through the baseplate and through the motor by a fan in front of the armature and exhausted back through the baseplate. This airflow removes the heat dissipated by the motor without circulating room air through the optical path. The amount of heat dissipated by the motor is reduced by operating it at 80 V ac. This reduction in operating voltage also reduces the amount of vibration generated by the synchronous motor without changing its speed.

CO_2 SYSTEM

The source is imaged by spherical mirror M51 through a set of gas correlation cells onto aperture A54, which is mounted on window W51. The source energy transmitted by A54 is imaged by spherical mirror M55 through the sample cell and onto the plane of window W53. This energy is collected by spherical mirror M58 and directed onto photodetector D51 through bandpass filter F51. The passband of this interference filter is centered at about 4.405μm (2270 cm^{-1}). The width of the passband between the 1/2 maximum transmittance points is about 0.044μm (22 cm^{-1}). The passband includes most of the P-branch of the ν_3 absorption band of the $^{13}C\ ^{16}O_2$ isotope. Photodetector D51 includes a PbSe element mounted on a single stage thermoelectric cooler.

Aperture A51, which is mounted on the face of M51, is imaged by mirror M55 onto the plane of window W52. Aperture sizes, focal lengths, and dimensions were adjusted such that the image of A51 on W52 is the same size as the image of A54 on W53. These images are smaller than the inside diameter of the sample cell. The 4 cm long sample cell has the same inside diameter as the 20 cm cell. The image of A51 on W52 is re-imaged by M58 onto the photodetector.

Both window W1 and mirror M52 are mounted in the wall of the correlation cell chamber near the source assembly. This wall has also been relieved to allow for thermal expansion without affecting the adjustment of M52. Further, M52 is shielded from direct source radiation by a wall of the source assembly. Apertures A52 and A53 minimize scattered energy, and

aperture A54 is overfilled to increase the stability. The limiting apertures of this system are A51 and A54.

It is expected that the 4 cm long sample cell will be used for samples taken directly from automotive exhaust and that the 20 cm long sample cell will be used for samples taken from diluted automotive exhaust. The sample cell in use is selected with a lever from the outside of the optics enclosure. The cells are spring loaded against metal stops to maintain the correct position and alignment. The sample gas flows through the 4 cm sample cell before flowing through the 20 cm sample cell. The flow is directed through the shorter cell first to allow observance of abrupt changes in gas concentration before mixing can occur in the longer cell. The gas flow is directed near the cell windows to prevent volumes of stagnant gas at the ends of the sample cells.

CO and CH_4 SYSTEMS

General

The CO and CH_4 detection systems are discussed together since most of the component parts and optical ray paths are common to both systems. The specific spectral passbands employed are controlled by the grating filter assembly in combination with an interference filter near each photodetector. These passbands were selected and adjusted to give a large throughput, good sensitivity to the gas being detected, and a very low sensitivity to other gases that might be in the sample gas. The passband of the CH_4 system is centered at about 3.315μm (3017 cm^{-1}). The width of the passband between the 1/2 maximum transmittance points is about 0.0176μm (16 cm^{-1}). The passband is almost centered on the Q-branch of the 3.3μm absorption band of CH_4. The passband of the CO system is centered at about 4.605μm (2171 cm^{-1}), with a width of about 0.0913μm (43 cm^{-1}). This passband includes absorption lines R1 through R12 of the fundamental absorption band of CO.

As in the CO_2 system, two sample cell lengths are employed to extend the useful range of sensitivities of the CO and CH_4 systems. Both sample cells are active at all times. The existing set of electronics can be switched between the outputs of the photodetector preamplifiers with switches on the electronics units. With this optical system it would be possible to add an electronic automatic range switching device to control the cell length in use. Alternately, the outputs of the photodetectors used with both cell lengths can be monitored simultaneously for flowing gas samples which have rapid and very large fluctuations in the gas concentration. About 75 percent of the radiant energy transmitted by the grating-filter assembly is directed through the 100 cm sample cell. The remaining 25 percent is directed through the 10 cm sample cell. This division of energy is based on the signal-to-noise requirements of the system.

Source Optics and Grating Filter Assembly

The spectral passbands of both the CO and the CH_4 systems are set by the grating-filter assembly. This grating monochromater forms an undispersed image of the entrance slit, S1, on the exit slit, S4, of the unit.

The source is imaged by mirror M1 through a pair of gas correlation cells onto slit S1. The energy transmitted by S1 is collimated by spherical mirror M11 and directed to the plane diffraction grating G. The grating is overfilled and acts as a limiting aperture. Part of the energy that is dispersed by the grating is collected by spherical mirrors M12 and M13. These mirrors form many dispersed monochromatic images of S1. Radiant energy near 4.6 μm is focused onto slit assembly S2 by mirror M12. Similarly, energy near 3 μm is focused onto slit assembly S3 by mirror M13.

Figure 6 shows an expanded view of slit assemblies S2 and S3. The energy is reflected vertically from the bottom mirror through the slit, and reflected from the top mirror back to the corresponding mirror M12 or M13. The dispersed energy that is transmitted by S2 and S3 is de-dispersed upon the second pass through the grating G. Mirror M11 forms an undispersed image of the entrance slit S1 onto the exit slit S4 through flat mirror M14. Slits S1, S2 and S3, and S4 are conjugate to each other. The spectral widths of the two passbands are set by the widths of S2 and S3. The center wavelengths of the passbands are set by the angular locations of S2 and S3. The slopes of each side of the passbands are set by the widths of the images of either S1 or S4 on S2 and S3. Slit S1 was made slightly wider than S4 to simplify alignment, thus the slopes are set by the image of S4, which lies within the bounds of S1.

The central ray of the energy transmitted by S4 is below the central ray transmitted by S1. These rays are parallel to each other and to the optics assembly baseplate. The central rays converge from M11 to the center of the grating where they cross. They are divergent from the grating to slit assemblies S2 and S3. The limiting apertures of the grating-filter assembly are slits S2, S3, S4, and the grating G. Apertures A1, A11, A12, and A13 reduce the scattered energy.

The grating-filter assembly transmitts undispersed radiant energy at multiple orders of the desired spectral passbands. Interference filters are used to limit each passband to a single order of the grating. A pair of these narrow bandpass filters are located near the photodetectors of each channel. This restricts the amount of ambient radiation reaching the photodetectors. One of these filters is also used as a dichroic mirror to separate the 4.6 μm radiant energy from the 3 μm radiant energy.

The components in the grating-filter assembly are enclosed within a dust-proof chamber. The base of this chamber serves as the mounting

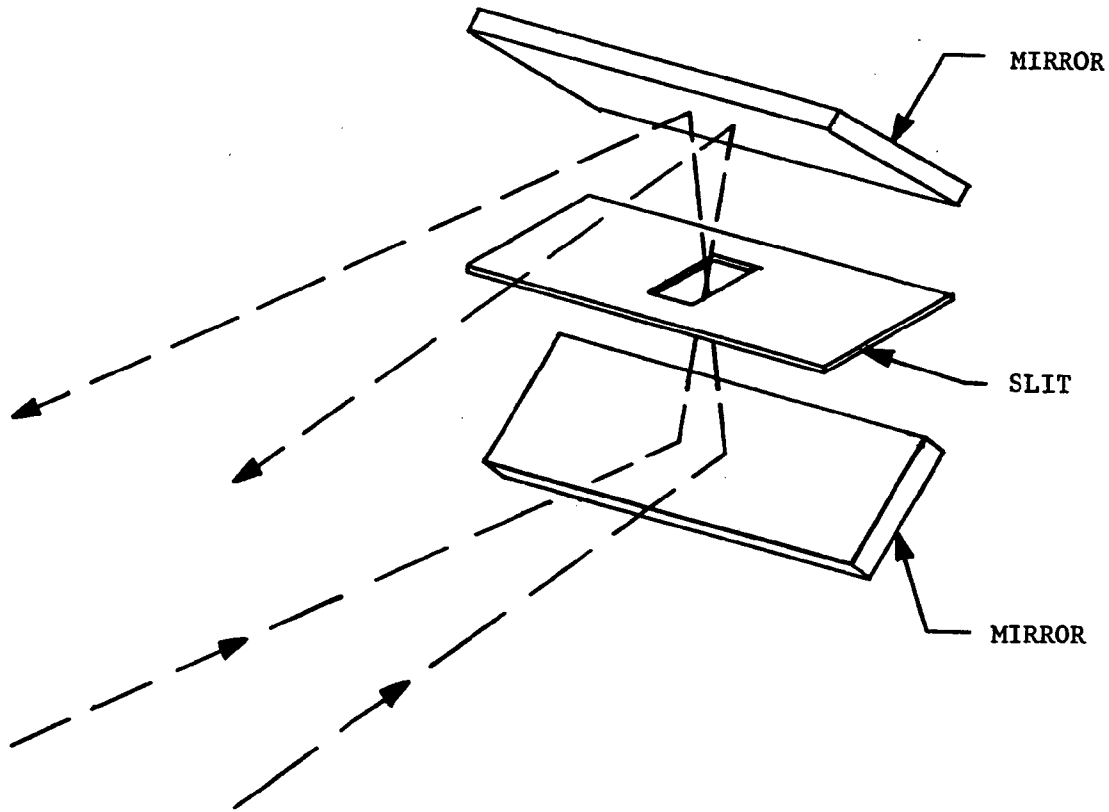

Figure 6. Expanded view of slit assembly S2 or S3. Many monochromatic images of the entrance slit S1 are formed on slits S2 and S3.

platform for these components. This chamber is, in turn, mounted on three spring loaded points against the optics assembly baseplate. A ball and spring-loaded-post maintain correct alignment between the grating-filter assembly and the remainder of the optics assembly. This mounting technique isolates the grating-filter assembly from stresses that may be applied to the optics assembly baseplate. This isolation assures stable wavelength passbands for the CO and the CH_4 systems.

Sample Cell and Photodetector Assemblies

The optical path length between the short sample cell entrance and exit windows W21 and W32 is 10.0 cm. The radiation that exits through the lower 25 percent of slit S4 is intercepted by flat mirror M31 and directed to spherical mirror M33. An image of mirror M11 is formed on the entrance window W21 of the sample cell. An image of slit S4 is formed on photodetectors D31 and D32. Interference filter F31 reflects 3 μm energy and transmits radiant energy near 4.6 μm. Interference filters F31 and F32 are bandpass filters that select a single order of the energy transmitted by the grating-filter assembly. They also reduce the amount of scattered energy reaching the photodetectors.

The optical path length of the double-passed sample cell is 100.0 cm The energy that exits through the upper 75 percent of slit S4 is collected by spherical mirror M21. The top edge of mirror M31 defines the lower boundary of slit S4 as viewed from mirror M21. Both M31 and S4 are mounted on window assembly W12 to maintain stable slit dimensions. An image of mirror M11 is formed on window W21 by spherical mirror M21. Similarly, an image of S4 is formed on mirror M23 by mirror M21. Spherical mirror M23 forms another image of M11 beside the image of M11 on W21. The image of S4 on M23 is re-imaged on photodetectors D21 and D22 by spherical mirrors M24 and M25, respectively. Interference filters F21 and F22 serve the same functions as filters F31 and F32. Photodetectors D21, D22, D31, and D32 include PbSe elements which are mounted on two-stage thermoelectric coolers.

The sample cell windows and end mirrors are easily removed for cleaning. The windows are bonded to flanges. The end mirror is covered by a metal cap. Rubber "O" ring seals with metal-to-metal contact between the cell and the end cap or window flanges provide a gas tight unit. Similar construction is used for the windows on the CO_2 sample cells. Mirror M23 is self-aligned by spring loading it against three points that contact the front spherical surface. The sample cell temperature may differ from the baseplate temperature as a result of the sample temperature. The sample cell is held rigidly to the optics baseplate near W21. The other end of the cell is allowed to move along the cell axis. This allows for stress-free differential thermal expansion of the cell. Mirror M23 is mounted to the sample cell. Since the cell is mounted to the baseplate near W21, which is near the center of curvature of M23, the alignment is insensitive to small movements of the sample cell relative to the baseplate.

Apertures A21, A22, and A23 reduce the amount of scattered energy that can reach the photodetectors. In addition, A21 protects the surfaces of M21 and M22 during the removal and reinstallation of window W21.

The sample gas coming from the CO_2 cells flows into and through the 10 cm cell and then into the 100 cm cell. It is exhausted from the system after flowing lengthwise through the 100 cm cell. The sample is directed through the shorter cell first to allow the observance of abrupt changes in gas concentration before any mixing can occur in the longer cell. Although not shown in the figure, a small portion of the sample gas flows into the cell near W21. This prevents the possible formation of a stagnant pocket or eddy of gas near W21. Similarly, although most of the sample is exhausted from the cell just in front of M23, a small flow of gas is exhausted from behind M23. This prevents the small volume between M23 and the cell end cap from containing stagnant gas that could contaminate samples added later.

SECTION IV

ELECTRONICS

GENERAL DESCRIPTION

The electronics for the three-channel gas correlation spectrometer were designed for good stability and low noise while preserving a reasonably small package size and weight. The photodetector is the limiting noise source in each channel. Component selection was limited to off-the-shelf items. The system was designed to operate within a laboratory at room temperature. To minimize costs, the electronics for each of the three channels are as much alike as possible.

A block diagram of the electronics for a single channel is presented in figure 1. The photodetector output consists of a 360 Hz carrier modulated at 30 Hz. The ratio of the modulation amplitude to the carrier amplitude is directly proportional to the amount of gas within the sample cell. Phase locked synchronous demodulation of the 30 Hz signal offers the best system signal-to-noise. The 30 Hz reference required for synchronous demodulation of the 30 Hz signal is also employed to synchronously modulate the carrier as necessary to cancel any residual 30 Hz modulation on the carrier when no sample is present.

The three electronics units and the power supply unit are mounted in a standard 19-inch (48.3 cm) electronics rack. The front panel heights are 8.75 inch (22.2 cm) for each electronics unit and 7 inches (17.8 cm) for the power supply unit. Line power is furnished through a single junction box within the electronics rack to prevent possible ground loops between systems. The power supply unit is mounted in the top of the electronics rack to prevent the heat dissipated from this unit from unnecessarily heating the other units. The front panels of the power supply unit and one of the electronics units are presented in figure 7. The signal and power cables that connect the optics assembly to the electronics unit are about 3.5 meters long.

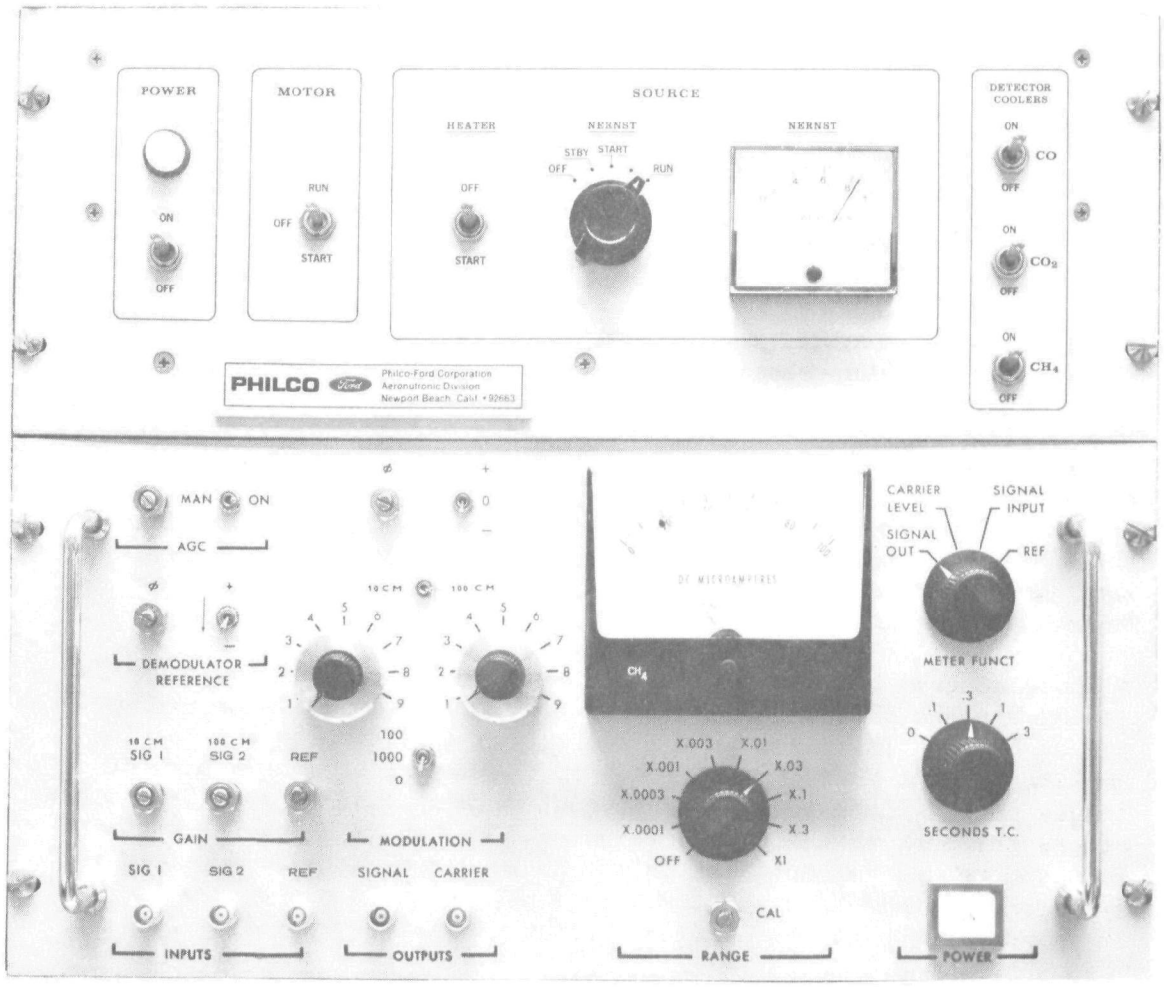

Figure 7. Power supply unit above a single electronics unit.

OPTICS UNIT

A schematic illustration of the electronics contained within the optics assembly that are used by a single signal channel of the system is presented in figure 8. The gain of each preamplifier is set to effect a carrier signal amplitude that is about 1 V peak-to-peak. Five photodetectors and preamplifiers are used for the three channel system.

A 45 V dc battery pack supplies the bias voltage to the photoconductive PbSe detectors. Jacks allow monitoring of the battery voltage in both the load and the no-load conditions. The total current drain from the bias battery by the photodetectors is about 40 μA when the photodetectors are thermoelectrically cooled. This should allow a battery life in excess of six months. A low-pass filter with a 1.1 second time constant in each channel prevents a possible crosstalk between channels as a result of coupling through the bias voltage supply. This filter also reduces any noise generated by the bias supply. A diode in series with the battery protects the electrolytic filter capacitors from damage that could occur if the battery polarity is reversed. A capacitor across the diode lowers the impedance of the protection circuit. The batteries are contained within a fluid tight chamber to prevent possible contamination of the optics system with battery electroyte.

The 30 Hz reference pickup shown in figure 1 consists of a light emitting diode (LED) and a phototransistor used in the common emitter mode. The beam of light between the LED and the phototransistor is chopped at 30 Hz by a single-blade chopper mounted on the correlation-cell shaft. The output impedance is about 490 Ω and the amplitude of the reference signal is about 400 mv peak-to-peak.

The reference system is supplied with -15 V dc from a power supply in an electronics unit. The photodetector preamplifiers are supplied with +15 and -15 V dc from the same power supply. Separate cables connect the reference and the preamplifier systems to the electronic unit power supply. Further isolation between systems is accomplished with resistance-capacitance filters that are installed next to the reference pickup and the preamplifiers.

POWER SUPPLY UNIT

The Nernst source, source heater, and the correlation cell drive motor receive their 60 Hz power from the power supply unit. The source current is controlled at the power supply unit and is displayed on a front panel meter. The amount of current that flows through the source is limited by either one, two, or three ballast tubes that are switched

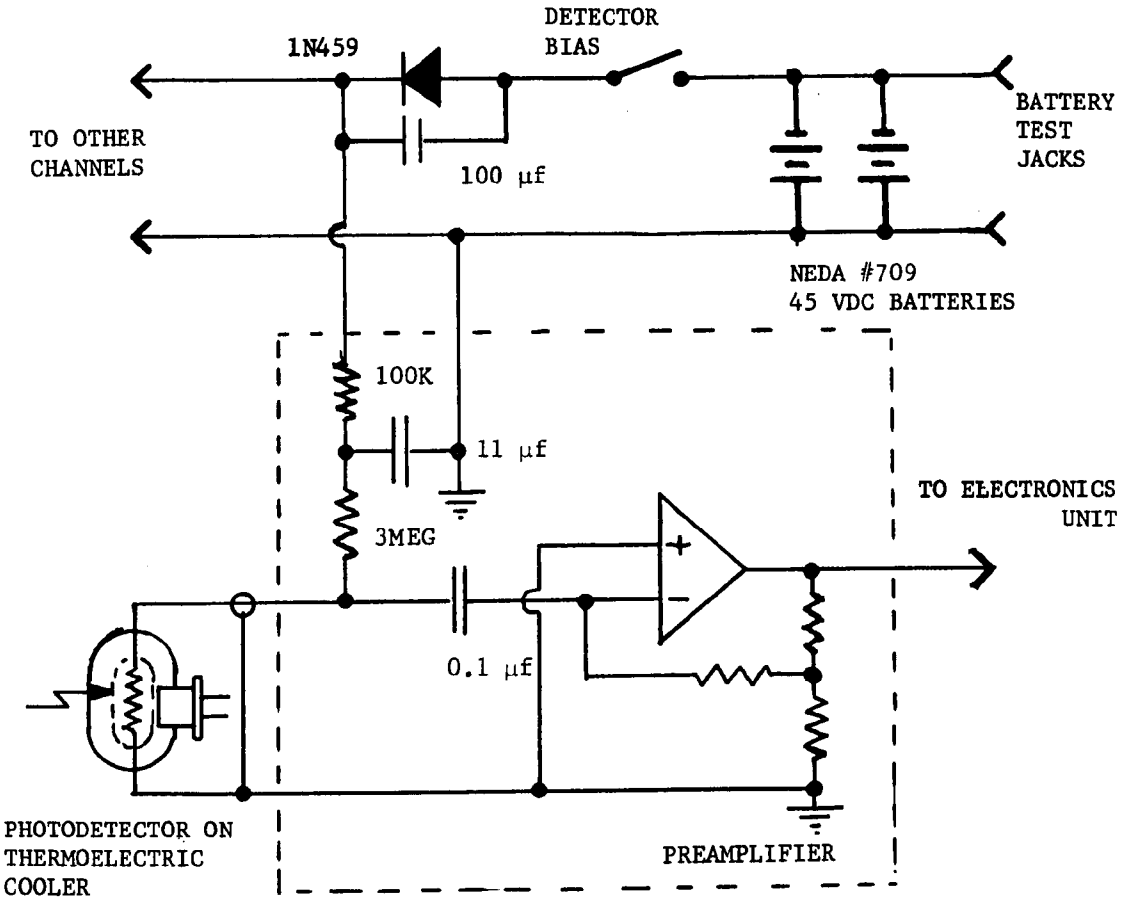

Figure 8. Schematic illustration of a single channel of the photodetector electronics within the optics assembly.

in parallel between the source and the 115 V ac power line. The fan that cools the Nernst source is controlled by this same switch. The fan is operated at 115 V ac except in the standby (STBY) mode when its voltage is reduced to about 70 volts. This approximately halves the fan speed. The source heater is supplied from a 60 V ac transformer in the power supply unit when the spring loaded source start switch is held on. In normal operation, the synchronous 1800 rpm motor is powered by 80 V ac supplied by a transformer in the power supply. The motor voltage is 115 V ac when the spring-loaded motor switch is held in the start position. The thermoelectric coolers for the photodetectors are powered from a 5 V dc power supply mounted in the power supply unit. A 3 Ω power resistor in series with each thermoelectric cooler converts the fixed-voltage supply to a fixed-current supply. Each of the five coolers draws about 1.8 amperes.

ELECTRONICS UNIT

General

Each of the three gas channels employs an electronics unit to process the detector signals. A functional block diagram of a single unit is presented in figure 1. The electronic unit is subdivided into a 30 Hz reference section, 360 Hz carrier section, and a 30 Hz signal section. Most of the electronics for these sections are contained on plug-in circuit cards with one card for each section. The circuit cards are interchangeable between the three electronics units. The differences among the three units are in the front panel controls. These differences reflect the use of a single photodetector for the CO_2 system and a pair of photodetectors for the CH_4 and CO systems. Switching between photodetector preamplifiers is accomplished with a toggle switch on the front panel of the electronics unit. Figure 7 illustrates the front panel controls for a unit for use with either the CO or the CH_4 systems.

Reference Section

The reference section of the unit is used to amplify, phase shift, and transform the signal from the reference pick-up into a form compatible with the remainder of the electronics unit. The input reference signals are amplified to a set level by the first stage of the reference section. The gain of this amplifier is adjusted by the operator and is not critical. The reference signals are then further amplified by a tuned amplifier with a Q of 5. This amplifier is followed by two adjustable phase shifters connected in series. The second phase shifter thus tracks any adjustment made in the first one. The phase shifters are used to obtain the proper phase between the reference and the photodetector signal. The phase can be adjusted easily without test equipment and should remain stable. The output stages of the phase shifters transform the sinusoidal reference signals into large amplitude square wave reference signals that drive the gates of field effect transistor (FET) switches in the modulation balance assembly and in the 30 Hz synchronous demodulator.

Carrier Section

The 360 Hz carrier signal section amplifies and normalizes the signals to a constant average carrier level. This section is also employed to balance out erroneous signals that can result from an imbalance in the transmissivities of the correlation cells.

The input signal from the photodetector preamplifier is amplified with a bandpass amplifier. The Q is about 3.5 and the center frequency is 360 Hz. The operator sets the gain control potentiometer of this amplifier to effect an indicated signal level that is near midscale on the front panel meter when the sample cell is filled with clean air. The adjustment is not critical since the automatic gain control (AGC) has a dynamic range of more than 5 to 1. The gain controlled stage of the AGC follows the tuned amplifier.

The modulation balance assembly follows the gain controlled amplifier. This assembly consists of an adjustable voltage divider and an FET switch that shunts part of the carrier signal to ground when the switch is closed. The FET switch is activated at 30 Hz by the reference system. This results in a square wave modulation at 30 Hz of the 360 Hz carrier. The voltage divider is adjustable to allow the FET to shunt up to 10 percent of the carrier signal to ground when the switch is closed. The adjustable system includes two potentiometers mounted on coaxial shafts. One potentiometer is for fine adjustments, the other for coarse adjustments. The adjustment resolution of the system is $\pm 2 \times 10^{-5}$ of the carrier amplitude. A front panel mounted switch allows the modulation balance system to be turned on and off. This three position switch also allows the inserted modulation to be either in phase or 180 degrees out of phase with the 30 Hz signal modulation.

The 360 Hz carrier demodulator follows the modulation balance assembly. The demodulation is performed by a precision full-wave rectification circuit.

The average demodulator output voltage is compared with a fixed reference voltage by the AGC control amplifier. Any error between the two voltages is coupled back to the gain controlled amplifier with a feedback loop. The closed loop response time constant is one second. Shorter time constants would remove an excessive amount of the 30 Hz signal modulation from the carrier. Longer time constants would increase the fractional error in the 30 Hz signal modulation that could occur due to large abrupt changes in transmissivity of the sample gas. The output of the carrier demodulator can be monitored on the panel meter and can be recorded from the carrier output jack. The AGC can be turned off with a switch on the front panel. The gain of the gain controlled amplifier is then set by a potentiometer that is mounted

beside the switch. With the AGC off, the 360 Hz system output is a measure of the sample gas transmissivity over the spectral bandpass of the system.

When the manual gain control is set to effect the same average carrier level as is maintained by the AGC, then the sensitivity of the 30 Hz system to small concentrations of sample gas is the same as when the AGC is operating. With this gain setting, the operator can block the radiation between the source and the photodetector to observe the character and the relative amplitude of the noise generated by the photodetector and the electronics systems.

Signal Section

The 30 Hz section of the unit amplifies and isolates the 30 Hz signal modulation. This is performed with a phase locked synchronous amplifier and demodulator tuned to 30 Hz. The demodulated output of the carrier serves as the input to the 30 Hz signal section. Much of the 720 Hz ripple that results from the 360 Hz demodulation process is removed by a three-stage low-pass filter.

The range switch is a stepped attenuator that sets the signal output range. The signal gains of the attenuator are X1.0, X0.3, X0.1, . . ., X0.0001, and off. The off position is used in setting the zero output level of the 30 Hz system. A single curve of the sensitivity of the system to different amounts of sample gas can be drawn by normalizing the output signal V_a/V_c by the attenuator gain g. The calibration potentiometer is a variable gain control that follows the range switch. A calibration constant C_a is proportional to this gain. It is adjusted by the operator such that the system response curve of $V^* = (V_a/V_c)/(g\ C_a)$ versus gas concentration is in agreement with the indicated output for the calibration sample gas that is employed.

The calibration potentiometer is incorporated into the feedback loop of a high gain bandpass amplifier with a Q of 8. The signal is further amplified and conditioned before being demodulated. A notch filter in front of the demodulator reduces any 60 Hz modulation that might be present on the carrier. The synchronous demodulator only demodulates the 30 Hz portion of the signal that is in phase with the 30 Hz reference. Any residual 60 Hz signal is passed by the synchronous, phase-locked, demodulator as ripple and does not affect the smoothed signal output. An amplifier with an adjustable time constant smooths the demodulated signal before it is presented on the front panel meter or at the signal output jacks. The time constants available are 0, 0.1, 0.3, 1.0, and 3.0 seconds. In the 0 position the response time is limited to about 0.08 second by the combination of low-pass filters, notch filters, and bandpass amplifiers.

A meter mounted on the front panel of the electronics unit allows the operator to monitor the reference level, the input signal level, the carrier level, and the output signal level. The reference and input signal levels are adjusted to effect a mid-scale indication on the meter.

Identically labeled input and output jacks are provided on both the front and back of the electronics units. The jacks are wired in parallel. A 10 K Ω resistor is in series with each pair of output jacks. The outputs can be grounded without affecting the operation of the system. The full scale signal output is -1.0 volt. The normal carrier output is about -1.5 volts. Shunt resistors across the output jacks will reduce these voltages to match the ranges of low level recorders. For example, a 10 Ω shunt resistor will act as a voltage divider with the 10 K Ω resistor to reduce the full scale signal output from -1 volt to -1 millivolt.

For clarity, the above description was limited to a single channel of electronics. Since two different sample cell lengths are employed for each gas species, two separate modulation balance assemblies are included in each electronics unit. The CO and the CH_4 detection systems also employ two different photodetectors and preamplifiers for each gas species. Separate adjustable gain controls were provided for each signal input. Toggle switches are used to switch from the signal inputs and modulation balance assemblies used with the short sample cell to the corresponding ones for the long sample cells. This construction allows the operator to switch rapidly between the different sample cells without changing the settings of the signal input gains or the modulation balance assemblies.

SECTION V

TEST DATA

The sensitivity of the gas correlation spectrometer to various gases has been measured. Plots of the normalized output, V^*, versus the sample concentration are presented in figures 9, 10, and 11 for CO, CH_4, and CO_2, respectively. For a given gas concentration, the system output is a function of the setting of the calibration potentiometer and the range switch. Both of these controls adjust the gain of the 30 Hz system. The calibration controls were set to effect a full scale output of about -1 volt for sample gas concentrations of 100 ppm of CO, 50 ppm of CH_4, and 1% of CO_2 when the samples were in the long sample cells. With the AGC operating, the output of the system V_a/V_c was then normalized by the gain setting, g, of the range switch used for each measurement and plotted against the concentration of the sample gases. The ordinate of the curve V^* is equal to $(V_a/V_c)/(g\ C_a)$, where C_a is a calibration constant that is proportional to the gain of the calibration control.

The sample gases were prepared by diluting measured amounts of CO, CH_4, and CO_2 with N_2. Some of the samples contained both CO and CH_4 with the N_2 dilutant. The sample containers were evacuated before use to prevent contamination of the sample. The samples were mixed with a mechanical stirring device inside the sample tank. The sample gas flow rate through sample cells was regulated at 0.2 liters/minute while V^* was being recorded. This flow rate is fast enough to prevent adsorption or desorption of gas from the walls of the sample cell and the gas handling system from affecting the concentration of the sample gas. A slow flow rate also minimizes the amount of sample gas required for each data point. A much faster flow rate was used to flush an old sample out of the sample cell with a new sample to reduce the waiting time between measurements. The gas flow rate is limited by a needle valve in the input gas line. The flow exhausts from the sample cell to the atmosphere, thus the pressure within the sample cell is slightly over one atmosphere.

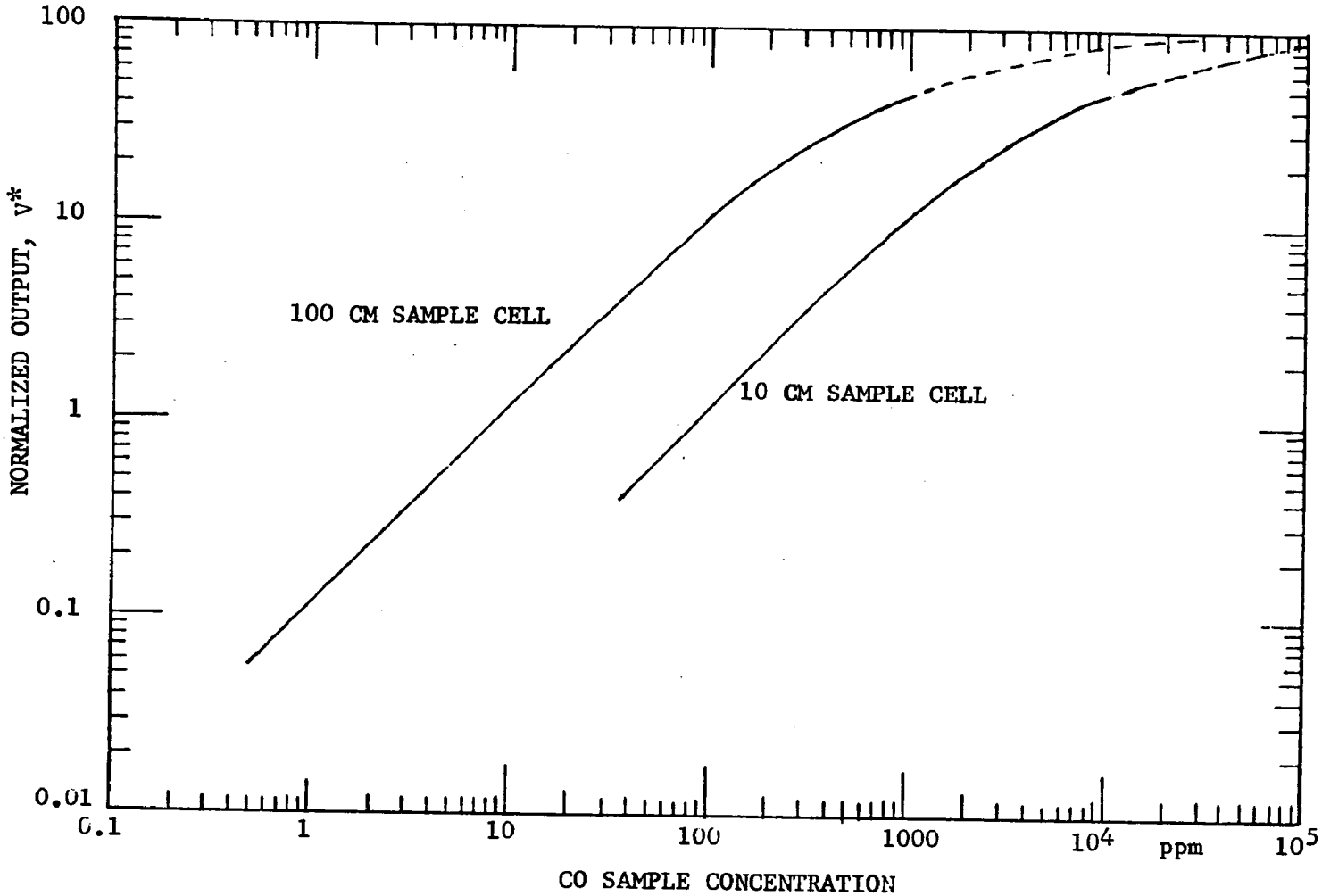

Figure 9. CO detection sensitivity.

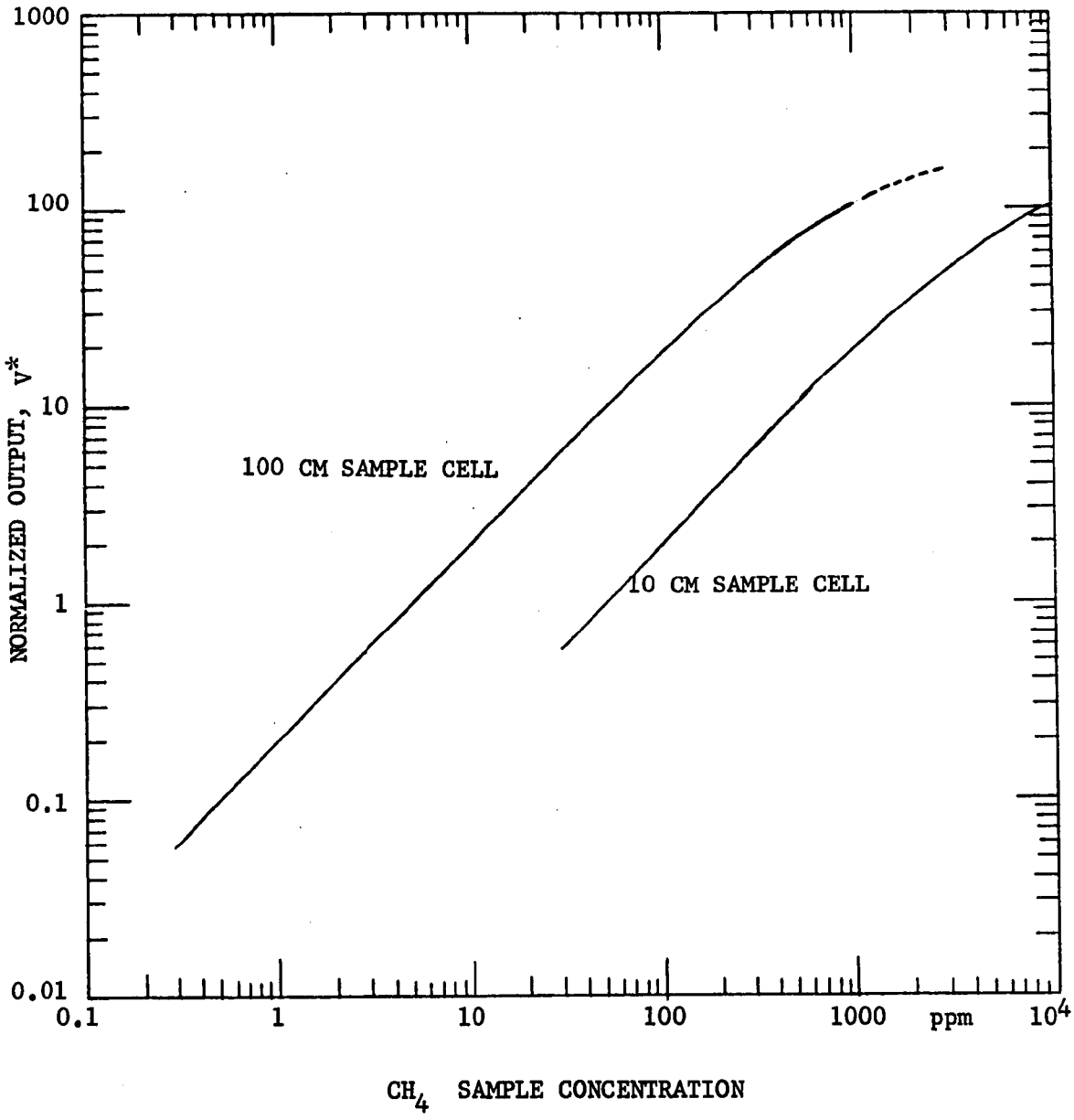

Figure 10. CH_4 detection sensitivity.

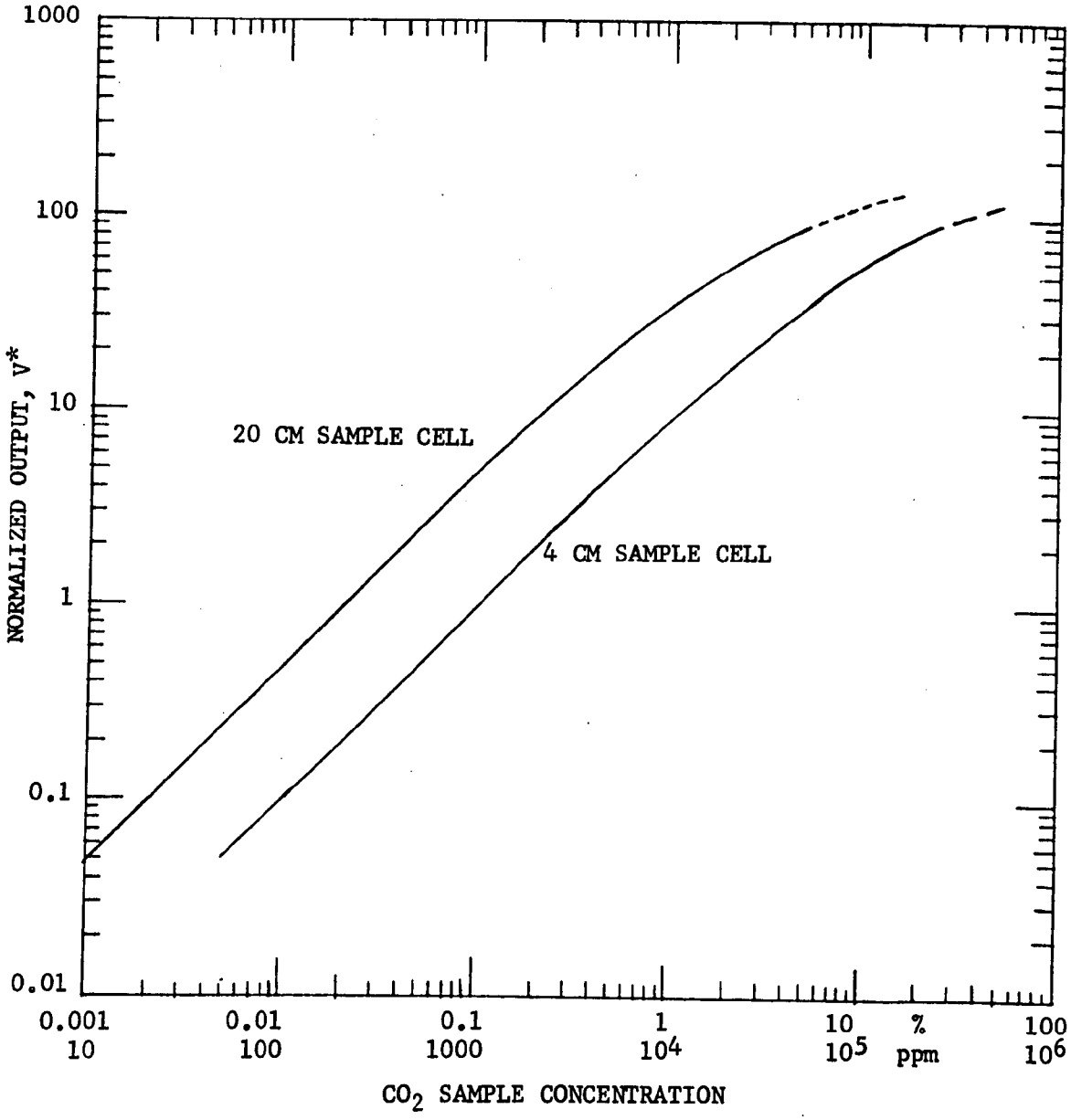

Figure 11. CO_2 detection sensitivity.

Two sensitivity curves are shown for each gas, one curve for each cell length. Both curves have the same shape but are displaced along the abcissa by the ratio of the cell lengths. The displacement results from the output being directly proportional to the product of the gas concentration and the sample cell length. This product is the absorber thickness at a given temperature and pressure. The useful measurement range is shown by the solid line portion of each curve. The lowest concentration indicated is the noise-equivalent-concentration (NEC) of the channel. The NEC is defined as the concentration that produces a signal equal to the peak-to-peak noise level. The upper limit of each measurement range is set by the concentration where the slope of the logrithmic curve is about 0.5. This correspondends to concentrations for which V^* is proportional to the square root of the concentration. Larger gas concentrations can be measured, but the accuracy decreases.

The ability of this system to measure small amounts of one gas in the presence of large amounts of other gas species is one of the main advantages of the gas correlation system. With the exception of water vapor, the system is insensitive to other gases in automotive exhausts. For typical exhaust gas concentrations, the error produced by the interfering gases was either less than the NEC or less than 1% of the amount of gas being measured. The discrimination ratio is given by the ratio of the amount of interfering gas to the error signal produced by the interfering gas. The system exhibits a discrimination ratio of 50,000 against H_2O by the CO system. This means that it takes a sample containing 50,000 parts of H_2O to produce the same signal as a sample containing 1 part of CO. The CH_4 system has a discrimination ratio of 13,000 against H_2O. A discrimination ratio with a negative sign means that the interfering gas produces a signal of opposite polarity to the signals produced by the gas species normally being detected. Since the error signal may not be directly proportional to the concentration of the interfering gas, discrimination ratios are measured with concentrations that are similar to those expected in automotive exhaust samples. Large concentrations of interfering gas may produce an unrealistically large discrimination ratio.

The discrimination ratios for several individual hydrocarbon species were measured by placing a pure sample of the interfering gas in a 0.1 cm long sample cell. This flow-through sample cell was located near the exit slit of the grating-filter assembly in the beam of radiation that traverses the 100 cm sample cell. The 100 cm sample cell was filled with N_2. A sample with a concentration of 1000 ppm in the 100 cm cell will produce the same output as the pure sample in the 0.1 cm cell. The use of pure samples simplifies the gas handling procedure. The hydrocarbon discrimination ratio is based on the required number of carbon atoms in the interfering gas to produce the same signal as a single carbon atom in a methane sample.

A hydrocarbon mixture was prepared by vaporizing 31.2 microliters of Indolene Clear 91 octane gasoline into a 47.3 liter tank containing N_2 at a pressure of 1.51 atmospheres. This lead free gasoline was analyzed by EPA on 11 May 1973. At one atmosphere pressure, the mixed sample contains 486 ppmc in N_2. This mixture in the 100 cm sample cell of the CH_4 analyzer produced an indicated output of -0.4 ppm of CH_4. This corresponds to a discrimination ratio of -1200. Adding 50 ppmc of ethylene and 50 ppmc of acetylene to this Indolene Clear mixture results in a hydrocarbon mixture that is representative of typical automotive exhaust minus the methane content. Increasing the carbon content of the Indolene Clear sample from 486 ppmc to 586 ppmc by the addition of ethylene and acetylene to the dilutant gas does not change the indicated output of the system. Thus, the discrimination ratio against typical exhaust minus methane is about -1450. This hydrocarbon mixture did not produce a detectable output on the CO_2 or the CO channels of the system.

Table 1 presents the noise levels of the system. Each channel is detector noise limited. The peak-to-peak noise for a 1 second time constant is expressed in terms of the NEC. The noise levels are approximately inversely proportional to the square root of the time contants. The NEC values for the short sample cells are larger than the NEC values for the long sample cells because the absorber thickness for a given gas concentration is less by the ratio of the cell lengths. Further, the optical throughput of the 10 cm sample cell is only about 1/3 of the throughput for the 100 cm sample cell and the photodetectors with highest detectivity were used with the long cells.

The gas analyzer system exhibits a slow drift in the zero signal output level which must be periodically corrected by the modulation balance control adjustment. The drift rate is rapid during the first few minutes of operation after turning on both the source and the motor. The drift rate decreases to a very small value after about 2 hours of warm-up operation. The zero-drift was less than the equivalent of 1 ppm of gas in the 100 cm sample cell for the CO and the CH_4 systems over a 2-1/2 hour period after a warm-up period of equal time. The average drift rate after this period was thus less than 0.4 ppm/hour.

Table 1. SYSTEM NOISE LEVELS

Gas	Cell Length (cm)	Time Constant (sec)	NEC (Noise-Equivalent Concentration) (peak-to-peak)	Normal Operating Range
CO	100	1	0.5 ppm	1 to 1,000 ppm
CO	10	1	35 ppm	100 to 10,000 ppm
CH_4	100	1	0.3 ppm	0.5 to 1,000 ppm
CH_4	10	1	30 ppm	100 to 10,000 ppm
CO_2	20	1	10 ppm (0.001%)	0.002 to 5%
CO_2	4	1	50 ppm (0.005%)	0.01 to 25%

SECTION VI

GLOSSARY OF SYMBOLS

A# - an aperture

ac - alternating current

AGC - automatic gain control

BB - a bearing block

C_a - calibration constant proportional to gain of calibration control

cm - centimeter

μm - micrometer

cm^{-1} - reciprocal centimeter, a wavenumber unit

CH_4 - methane

CO - carbon monoxide

CO_2 - carbon dioxide

D# - a photodetector

dc - direct current

F# - a filter

f_a - 30 Hz correlation cell frequency

f_c - 360 Hz carrier frequency

FET - field effect transistor

g - relative gain of 30 Hz signal attenuator

G - a plane diffraction grating

GC1 - gas correlation cell containing CO and CH_4

GC2 - gas correlation cell containing N_2 and a neutral attenuator

GC3 - gas correlation cell containing CO_2

GC_4 - gas correlation cell containing N_2 and a neutral attenuator

Hz - Hertz

KΩ - kilo ohms

Ω - ohms

LED - light emitting diode

M# - a mirror

mV - millivolt

N_2 - nitrogen

NEC - noise equivalent-concentration: the gas concentration that will produce the same output signal as the peak-to-peak noise level

PbSe - lead selenide

ppm - parts per million

ppmc - parts per million of carbon

Q - measure of bandpass of a tuned circuit

rpm - revolutions per minute

S# - a slit

T_1 - transmittance of GC1

T_2 - transmittance of GC2

T_{co} - T_{sam} when sample gas is CO

T_{sam} - transmittance of sample gas

T_χ - T_{sam} when sample is some interfering gas

V - Volt

V^* - normalized output $(V_a/V_c)/(g\ C_a)$

V_a - 30 Hz signal amplitude

V_c - average 360 Hz carrier amplitude

W# - a window

% - percent

ν - wavenumber

ν_a - wavenumber at the center of an absorption line

$\Delta\nu$ - bandpass expressed in wavenumbers

ABBREVIATED LABELS ON CONTROLS

AGC - automatic gain control

CAL - calibrate

FUNCT - function

MAN - manual gain, the AGC is turned off

REF - reference

SIG - signal

STBY - standby

T.C. - time constant

ϕ - phase

SECTION VII

PATENT INFORMATION

Follwoing are two (2) inventions which have been declared as subject inventions:

Name of Inventor	Title of Invention	Patent Application Serial No. and/or Contractor Disclosure No.
Dr. Darrell E. Burch, Francis J. Gates, David A. Gryvnak, and John D. Pembrook	Gas Analyzer, Employing a Grating and a Gas Selector Cell	33-059 (A-73-07)
Dr. Darrell E. Burch, Francis J. Gates, David A. Gryvnak, and John D. Pembrook	Gas Analyzer	31-154-A (A-71-29)

Philco-Ford is currently requesting that the Government waive title and retain only a non-exclusive royalty-free, irrevocable license in order that the Contractor may file for these inventions and pursue additional in-house work to further exploit their application in the public interest.

BIBLIOGRAPHIC DATA SHEET	1. Report No. EPA-650/2-73-030	2.	3. Recipient's Accession No.
4. Title and Subtitle Instrument to Monitor CH_4, CO, and CO_2 in Auto Exhaust.			5. Report Date October 1973 6.
7. Author(s) D. E. Burch and J. D. Pembrook			8. Performing Organization Rept. No.
9. Performing Organization Name and Address Philco-Ford Corporation Aeronutronic Division Ford Road Newport Beach, California 92663			10. Project/Task/Work Unit No. 11. Contract/Grant No. 68-02-0587
12. Sponsoring Organization Name and Address EPA, Chemistry and Physics Laboratory, National Environmental Research Center Research Triangle Park, North Carolina 27711			13. Type of Report & Period Covered Final Report 14.

15. Supplementary Notes

16. Abstracts

An infrared analyzer employing gas cell correlation techniques and thermoelectrically-cooled photodetectors has been designed and constructed to measure the concentrations of methane, carbon monoxide, and carbon dioxide in automotive exhausts. The dynamic range from the minimum detectable concentration to the maximum concentration that can be measured accurately for each gas is: methane, 0.3 ppm to 10,000 ppm, carbon monoxide, 0.5 ppm to 10,000 ppm, and carbon dioxide, 10 ppm to 250,000 ppm. The wide dynamic range is made possible by employing two different sample cell lengths for each gas. The concentrations of the three gases are measured simultaneously and independently. Discrimination against other gases in the automotive exhaust is very good.

17. Key Words and Document Analysis. 17a. Descriptors

Air pollution
Measuring instruments
  Infrared spectrophotometers
Exhaust gases
  Methane
  Carbon dioxide
  Carbon monoxide

17b. Identifiers/Open-Ended Terms

Air pollutant measuring equipment
Gas correlation spectrophotometer

17c. COSATI Field/Group 13B, 7B, 7C

18. Availability Statement	19. Security Class (This Report) UNCLASSIFIED	21. No. of Pages 46
	20. Security Class (This Page UNCLASSIFIED	22. Price

FORM NTIS-35 (REV. 3-72) USCOMM-DC 14952-P72